

# Design and Synthesis of Laser-Activatable Tetrazoles for a Fast and Fluorogenic Red-Emitting 1,3-Dipolar Cycloaddition Reaction

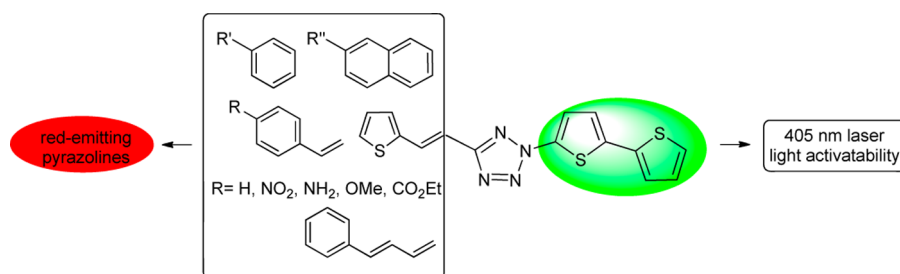
Peng An, Zhipeng Yu, and Qing Lin\*

Department of Chemistry, State University of New York at Buffalo, Buffalo, New York  
14260-3000, United States

qinglin@buffalo.edu

Received September 13, 2013

## ABSTRACT



The design and synthesis of a new class of laser light activatable tetrazoles with extended  $\pi$ -systems is reported. Upon 405 nm laser light irradiation, these bithiophene-substituted tetrazoles underwent extremely fast 1,3-dipolar cycloaddition reactions with dimethyl fumarate with second-order rate constants approaching  $4000 \text{ M}^{-1} \text{ s}^{-1}$ . The resulting pyrazoline cycloadducts exhibited solvent-dependent red fluorescence, making these tetrazoles potentially useful as fluorogenic probes for detecting alkenes *in vivo*.

Biomolecular imaging with fluorophores allows real-time monitoring of cellular processes with high spatial and temporal resolution. Compared with fluorescent proteins, chemical fluorescent probes are less likely to perturb the biological process under study because of their small sizes and tunable photophysical properties.<sup>1</sup> To minimize the interference caused by autofluorescence, environment-sensitive fluorescent probes with emissions in the red or near-infrared region are highly desirable for diverse applications in living systems,<sup>2</sup> including detecting protein

localization,<sup>3</sup> probing protein electrostatics,<sup>4</sup> and studying protein conformations.<sup>5</sup>

Recently, we reported the *in situ* formation of pyrazoline fluorophores for labeling proteins in living cells *via* a photoinduced tetrazole–alkene cycloaddition reaction ('photoclick' chemistry).<sup>6</sup> Compared with direct fluorophore attachment, the advantages of our photoclick chemistry approach include the following: (i) a fluorophore can be formed at any desired location within a protein of interest through the use of the amber codon suppression technique; (ii) the fluorogenic nature of the reaction allows fluorescent imaging without the washing step; and (iii) the necessary photoinduction step offers spatiotemporal

(1) Lavis, L. D.; Raines, R. T. *ACS Chem. Biol.* **2008**, *3*, 142.

(2) (a) Egawa, T.; Hirabayashi, K.; Koide, Y.; Kobayashi, C.; Takahashi, N.; Mineno, T.; Terai, T.; Ueno, T.; Komatsu, T.; Ikegaya, Y.; Matsuki, N.; Nagano, T.; Hanaoka, K. *Angew. Chem., Int. Ed.* **2013**, *52*, 3874. (b) Sun, W.; Fan, J.; Hu, C.; Cao, J.; Zhang, H.; Xiong, X.; Wang, J.; Cui, S.; Sun, S.; Peng, X. *Chem. Commun.* **2013**, *49*, 3890. (c) Yuan, L.; Lin, W.; Yang, Y.; Chen, H. *J. Am. Chem. Soc.* **2012**, *134*, 1200. (d) Lukinavicius, G.; Umezawa, K.; Olivier, N.; Honigsmann, A.; Yang, G.; Plass, T.; Mueller, V.; Reymond, L.; Corr a, I. R., Jr.; Luo, Z. G.; Schultz, C.; Lemke, E. A.; Heppenstall, P.; Eggeling, C.; Manley, S.; Johnsson, K. *Nat. Chem.* **2013**, *5*, 132.

(3) Zhuang, Y.-D.; Chiang, P.-Y.; Wang, C.-W.; Tan, K.-T. *Angew. Chem., Int. Ed.* **2013**, *52*, 8124.

(4) Cohen, B. E.; McAnaney, T. B.; Park, E. S.; Jan, Y. N.; Boxer, S. G.; Jan, L. Y. *Science* **2002**, *296*, 1700.

(5) Cohen, B. E.; Pralle, A.; Yao, X.; Swaminath, G.; Gandhi, C. S.; Jan, Y. N.; Kobilka, B. K.; Isacoff, E. Y.; Jan, L. Y. *Proc. Natl. Acad. Sci. U.S.A.* **2005**, *102*, 965.

(6) (a) Song, W.; Wang, Y.; Qu, J.; Madden, M. M.; Lin, Q. *Angew. Chem., Int. Ed.* **2008**, *47*, 2832. (b) Song, W.; Wang, Y.; Qu, J.; Lin, Q. *J. Am. Chem. Soc.* **2008**, *130*, 9654. (c) Lim, R. K.; Lin, Q. *Acc. Chem. Res.* **2011**, *44*, 828.

control over the fluorophore generation. While we have endeavored to tune the photoactivation wavelength to the long-wavelength region,<sup>7</sup> including 405 nm laser light,<sup>8</sup> the emissions of the pyrazoline fluorophores are still restricted to cyan-to-green colors.<sup>9</sup> Therefore, the pyrazolines with the red to infrared fluorescence are highly desirable. To this end, here we report the design and synthesis of *N*<sup>2</sup>-bithiophene-substituted tetrazoles that can be activated by a 405 nm laser light and produce the red-emitting pyrazoline fluorophores upon fast cycloaddition reactions with dimethyl fumarate. Furthermore, we found that the *in situ* formed pyrazoline fluorophores showed solvent-dependent fluorescence, which may make them useful to probe the polarity change in biological systems.

In designing tetrazoles that yield red fluorescent pyrazoline cycloadducts, we considered the following recent findings: (i) the substitution of the bithiophene moiety at the *N*<sup>2</sup>-position of tetrazole gave rise to not only 405 nm photoactivatability<sup>8</sup> but also excellent cycloaddition reactivity;<sup>10</sup> and (ii) extended  $\pi$ -conjugation, particularly at the *C*<sup>5</sup>-position of tetrazole, modulates the fluorescence of the resulting pyrazolines. We hypothesized that the tetrazoles with a *N*<sup>2</sup>-bithiophene substituent and an extended  $\pi$ -system at the *C*<sup>5</sup>-position would generate red fluorescent pyrazoline cycloadducts upon cycloaddition with a suitable dipolarophile while at the same time retain 405 nm photoreactivity and fast cycloaddition reaction kinetics. Accordingly, we designed tetrazoles **1–9** incorporating these two features (Figure 1).

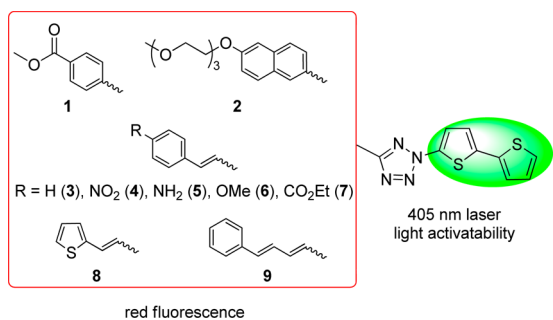


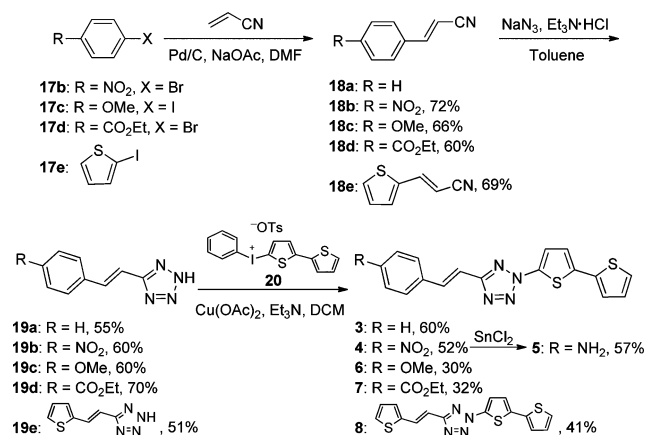
**Figure 1.** Tetrazole structures with bithiophene as a trigger for 405 nm photoreactivity.

Diaryltetrazoles **1** and **2** were synthesized using the cross-coupling method we reported recently<sup>8</sup> (Scheme S1). Separately, a convergent route was developed for the synthesis of styrenylaryltetrazoles **3–8** (Scheme 1). In brief, the substituted (*E*)-arylacrylonitriles **18b–e** were prepared

through the Heck-type cross-coupling between acrylonitrile and the various aryl halides **17b–e** with 60–72% yields. The nitriles were then converted to *2H*-tetrazoles **19a–e** in 51–70% yields by treating the arylacrylonitriles with NaN<sub>3</sub> in the presence of triethylammonium chloride in toluene. Tetrazoles **3–4** and **6–8** were obtained through the Cu<sup>II</sup>-catalyzed cross-coupling between tetrazoles **19a–e** and phenyl(bithiophen-2-yl)iodonium salt **20** with modest yields. The amine-substituted vinylaryltetrazole **5** was obtained in 57% yield by treating tetrazole **4** with SnCl<sub>2</sub> (Scheme 1).

The *trans,trans*-phenylbutadiene-substituted tetrazole **9** was constructed by the Wittig reaction according to Scheme 2. Briefly, cinnamyl alcohol **21** was converted to the corresponding phosphonium bromide **23** in 66% yield through successive treatment with CBr<sub>4</sub> and PPh<sub>3</sub>. The cognate aldehyde **27** was synthesized through a four-step procedure: (i) ethyl carbonocyanidate was reacted with NaN<sub>3</sub> to give tetrazole **25** in 70% yield; (ii) tetrazole **25** was treated with phenyl(bithiophen-2-yl)iodonium salt **20** in the presence of Cu(OAc)<sub>2</sub> to afford tetrazole **26** in 40% yield; (iii) reduction of **26** by LiAlH<sub>4</sub>; and (iv) oxidation with PCC generated aldehyde **27** in 90% yield over two steps. Finally, a Wittig reaction was carried out by treating phosphonium bromide **23** with *n*-BuLi followed by the addition of **27** to give (2-bithiophen-2-yl)-5-*trans,trans*-4-phenylbuta-1,3-dienyltetrazole **9** in 50% yield.

### Scheme 1. Synthesis of Tetrazoles 3–8



With tetrazoles **1–9** in hand, their UV–vis properties were measured (Figure S1) and the data are collected in Table 1. The maximum absorption wavelength ranges from 352 to 364 nm. Tetrazoles with the electron-donating groups (**5** and **6**) provide greater molar absorption coefficients than those with the electron-withdrawing groups (**4** and **7**). Subsequently, we examined the photoreactivities of the tetrazoles toward dimethyl fumarate, a symmetrical electron-deficient dipolarophile we used previously,<sup>8,12</sup> in PBS/ACN (1:1, v/v; PBS = phosphate buffered saline, pH 7.4) with photoirradiation by a diode laser (405 nm, 24 mW).<sup>13</sup>

(11) Wang, Y.; Vera, C. I.; Lin, Q. *Org. Lett.* **2007**, *9*, 4155.

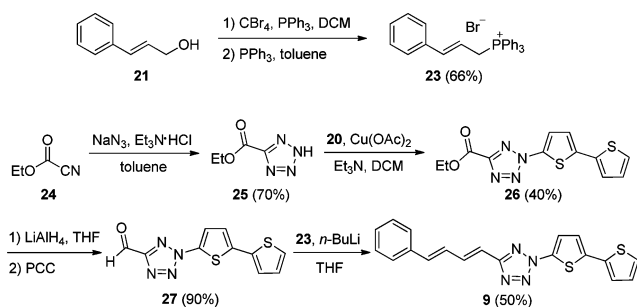
(7) (a) Wang, Y.; Hu, W. J.; Song, W.; Lim, R. K.; Lin, Q. *Org. Lett.* **2008**, *10*, 3725. (b) Yu, Z.; Ho, L. Y.; Wang, Z.; Lin, Q. *Bioorg. Med. Chem. Lett.* **2011**, *21*, 5033.

(8) An, P.; Yu, Z.; Lin, Q. *Chem. Commun.* **2013**, *49*, 9920.

(9) (a) Song, W.; Wang, Y.; Yu, Z.; Vera, C. I.; Qu, J.; Lin, Q. *ACS Chem. Biol.* **2010**, *5*, 875. (b) Yu, Z.; Pan, Y.; Wang, Z.; Wang, J.; Lin, Q. *Angew. Chem., Int. Ed.* **2012**, *51*, 10600.

(10) Wang, Y.; Song, W.; Hu, W. J.; Lin, Q. *Angew. Chem., Int. Ed.* **2009**, *48*, 5530.

## Scheme 2. Synthesis of Tetrazole 9



We found that tetrazoles **2**, **3**, **7**, and **8** gave clean conversions to the pyrazoline cycloadducts (Table 1) while tetrazoles **6** and **9** showed  $\geq 90\%$  yields along with small amounts of side products based on HPLC traces (Figure S2). Tetrazole **1** gave only 58% conversion with the remainder being the starting materials. Interestingly, tetrazoles **4** and **5** showed no reactivity despite their strong absorption at 405 nm (Figure S1). The lack of photoreactivity for the  $\text{NO}_2$ -containing tetrazoles, but not the ester-containing tetrazoles,<sup>7a</sup> was also observed in our previous studies.<sup>11</sup> On the other hand, tetrazole **5** was found to be weakly fluorescent, emitting the incident light as the fluorescence rather than breaking up the tetrazole ring.

To quantify tetrazole reactivity, we performed kinetic analyses by following the cycloaddition reactions of tetrazoles with dimethyl fumarate in quartz tubes under 405 nm laser irradiation with HPLC. The second-order rate constants,  $k_2$ , were determined (Figure S3), and the data are collected in Table 1. To our delight, tetrazoles **6**, **8**, and **9** showed extremely fast kinetics with  $k_2$  values approaching  $4000 \text{ M}^{-1} \text{ s}^{-1}$ , more than 3-fold faster than pure oligothiophene-based tetrazoles.<sup>8</sup> This is probably due to the HOMO-lifting effect (increases in the nitrile imine HOMO energies)<sup>10</sup> endowed by attachment of the extended electron-rich  $\pi$ -system to the *in situ* generated nitrile imine. Meanwhile, when the electron-withdrawing ester group was present, greater than 10-fold reduction in kinetic constant was observed ( $k_2 = 220$  and  $350 \text{ M}^{-1} \text{ s}^{-1}$  for tetrazoles **1** and **7**, respectively). In general, styrenylaryltetrazoles showed faster reaction kinetics than diaryltetrazoles (compare **1** to **7** and **2** to **6**). Remarkably, the potential intramolecular 1,3-dipolar cycloaddition reactions<sup>14</sup> among styrenylaryltetrazoles **3–8** and phenylbutadienylaryltetrazole **9** were not observed, presumably due to the geometric constraint posed by the *trans*-alkenes in these tetrazoles.

Next, the pyrazoline cycloadducts **10–16** were isolated and their photophysical properties are collected in Table 2.

(12) (a) Wang, J.; Zhang, W.; Song, W.; Wang, Y.; Yu, Z.; Li, J.; Wu, M.; Wang, L.; Zang, J.; Lin, Q. *J. Am. Chem. Soc.* **2010**, *132*, 14812. (b) Lim, R. K.; Lin, Q. *Chem. Commun.* **2010**, *46*, 7993.

(13) The light intensity value was recorded by placing a FieldMaster GS energy analyzer equipped with an LM-10 HTD power meter sensor in the light path of the laser beam.

(14) Yu, Z.; Ho, L. Y.; Lin, Q. *J. Am. Chem. Soc.* **2011**, *133*, 11912.

**Table 1.** UV–vis Absorption Properties of Tetrazoles **1–9** and Characterization of Their Reactivities in the 405 nm Laser Light Induced Cycloaddition Reaction<sup>a</sup>

tet	$\lambda_{\text{max}}$ (nm)	$\epsilon_{\text{max}}$ ( $\text{M}^{-1} \text{ cm}^{-1}$ )	pyrazoline	yield (%) <sup>b</sup>	$k_2$ ( $\text{M}^{-1} \text{ s}^{-1}$ ) <sup>c</sup>
<b>1</b>	352	18,600		58	$220 \pm 30$
<b>2</b>	356	26,200		98	$1,430 \pm 73$
<b>3</b>	354	27,700		97	$1,450 \pm 150$
<b>4</b>	362	22,400		ND <sup>d</sup>	/
<b>5</b>	364	31,100		ND <sup>d</sup>	/
<b>6</b>	356	32,400		92	$3,870 \pm 260$
<b>7</b>	356	22,400		95	$350 \pm 40$
<b>8</b>	360	26,400		95	$3,600 \pm 570$
<b>9</b>	358	46,500		90	$3,960 \pm 172$

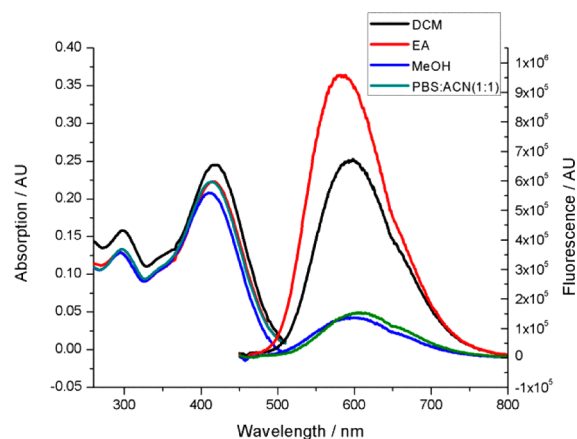
<sup>a</sup>For UV–vis measurement, tetrazoles were dissolved in PBS/ACN (1:1, v/v) to obtain concentrations of  $25 \mu\text{M}$ . For cycloaddition reactions, a solution of  $20 \mu\text{M}$  tetrazole and  $1 \text{ mM}$  dimethyl fumarate in  $1 \text{ mL}$  of PBS/ACN (1:1) in a quartz test tube was photoirradiated with 405 nm laser for 30 s. <sup>b</sup>Yields were determined by comparing the desired pyrazoline peak area in the HPLC trace to that of a pyrazoline control with known concentration. See Figure S2 in the Supporting Information for details. <sup>c</sup>Second-order rate constant of the cycloaddition; see Figure S3 in the Supporting Information for details. <sup>d</sup>The desired pyrazoline product was not detected; the tetrazole was found stable under the photoirradiation conditions.

**Table 2.** UV–vis Absorption and Fluorescence Properties of Pyrazolines **10**–**16**<sup>a</sup>

pyrazoline	$\lambda_{\text{max}}$ (nm)		$\lambda_{\text{em}}$ (nm) <sup>b</sup>		Stokes shift (cm <sup>-1</sup> ) <sup>c</sup>	$\Phi_f$ (%) <sup>d</sup>
	EtOAc	PBS/ACN	EtOAc	PBS/ACN		
<b>10</b>	425	425	596	630	6750	0.3
<b>11</b>	402	402	553	575	6790	1.5
<b>12</b>	416	416	582	612	6860	0.4
<b>13</b>	418	418	574	600	6500	0.4
<b>14</b>	437	437	610	644	6490	0.2
<b>15</b>	424	424	595	615	6780	0.3
<b>16</b>	435	432	608	620	6540	0.2

<sup>a</sup> Pyrazolines were dissolved in either EtOAc or PBS/ACN (1:1, v/v) to obtain concentrations of 10  $\mu\text{M}$ . <sup>b</sup>  $\lambda_{\text{ex}} = 405 \text{ nm}$ . <sup>c</sup> Based on the values measured in EtOAc. <sup>d</sup> Fluorescence quantum yields were determined in EtOAc using DAPI dye as a reference.

All pyrazoline cycloadducts showed bathochromic shifts in their absorption and emission maxima compared to diaryltetrazoles,<sup>7</sup> accompanied by large Stokes shifts (6490–6860  $\text{cm}^{-1}$ ; Table 2). All pyrazoline cycloadducts except **11** showed red fluorescence in PBS/ACN (1:1, v/v), and pyrazoline **14** even reached the near-infrared region with  $\lambda_{\text{em}}$  of 644 nm. However, the quantum yields of the pyrazoline fluorophores were rather low (0.2–1.5%), which can be attributed to their flexible structures and thus their strong tendency for nonradiative decay. Another observation was that the emission maxima of these pyrazolines depend critically on solvent polarity with significant hypsochromic shifts (12–34 nm) going from polar solvents to nonpolar ones, while the absorption spectra showed little change. As an illustration, pyrazoline **12** gave an emission maximum of 612 nm in polar PBS/ACN (1:1, v/v) solvent, but 582 nm in nonpolar EtOAc along with a concurrent increase in fluorescence intensity by more than 6-fold (Figure 2). This fluorescence intensity “turn-on” increased to 30-fold when organic cosolvent ACN in PBS/ACN decreased to 20% (Figure S4), suggesting that these red-emitting pyrazoline fluorophores may serve as environment-sensitive probes to detect polarity change in protein structures.<sup>3–5</sup>

**Figure 2.** UV–vis absorption (left) and fluorescence spectra (right) of pyrazoline **12** measured at 10  $\mu\text{M}$  in the various solvents. For fluorescence measurement,  $\lambda_{\text{ex}} = 405 \text{ nm}$ .

In summary, we have designed and synthesized a series of biaryl and styrenylaryl tetrazoles containing both a 405 nm photoactivatable bithiophene moiety and an extended  $\pi$ -system. The majority of these new tetrazoles participated in the laser-triggered photoclick reaction with dimethyl fumarate, giving rise to the red fluorescent pyrazoline cycloadducts with the fastest kinetics reported so far for the photoclick chemistry ( $k_2$  up to 3960  $\text{M}^{-1} \text{s}^{-1}$ ). Because the pyrazoline cycloadducts showed environment-dependent “turn-on” fluorescence, these new tetrazoles should offer a useful tool to study protein electrostatics and protein conformations involving changes in solvent accessibility and/or polarity.

**Acknowledgment.** We gratefully acknowledge the National Institutes of Health (GM 085092) for financial support. P.A. is a visiting graduate student from Lanzhou University sponsored by the China Scholarship Council.

**Supporting Information Available.** Supplemental figures, experimental procedure, and characterization of all new compounds. This material is available free of charge via the Internet at <http://pubs.acs.org>.

The authors declare no competing financial interest.